Calonne, N., F. Flin, S. Morin, B. Lesaffre, S. Rolland du Roscoat, and C. Geindreau (2011), Numerical and experimental investigations of the effective thermal conductivity of snow, *Geophys. Res. Lett.*, doi:10.1029/2011GL049234.

Numerical and Experimental Investigations of the Effective Thermal Conductivity of Snow

N. Calonne, F. Flin, S. Morin, B. Lesaffre, S. Rolland du Roscoat and C. Geindreau

Auxiliary Material

Calonne, N., F. Flin, S. Morin, B. Lesaffre, S. Rolland du Roscoat, and C. Geindreau (2011), Numerical and experimental investigations of the effective thermal conductivity of snow, *Geophys. Res. Lett.*, doi:10.1029/2011GL049234.

Table of Contents and General Information

Table of Contents

General Information

In the following, we provide the list and related information for all the samples used in this study. For each snow type [*Fierz et al., 2009*], a typical microtomographic sample is presented together with its main results in terms of effective thermal conductivity.

- **Figures S1a-S6a:** 3D images of the snow sample. The color coding of the images corresponds to the curvature field, which allows an easy representation of the 3D structure from planar images.

- **Figures S1b-S6b:** Estimations of the REV (the smallest fraction of the sample volume from which a variable representative of the whole can be determined) with respect to the thermal conductivity. It is estimated by calculating values of the thermal conductivity from several sub-volumes of increasing sizes. The REV is reached as soon as values remain constant when sub-volumes of calculations increase.

- **Tables S2-S7:** Numerical values of the diagonal terms of the effective thermal conductivity. For all the images of the study, the non diagonal terms are 100 times lower than the diagonal values and can be neglected.

List of the 30 Samples Used in the Study

Sample name	Snow type	Voxel size (μm)	Remarks	Main References
Fr	PP	4.91	Sampled at Col de Porte[1], 14 February 2002.	This study
I01	PP	4.91	Sampled at Col de Porte, 15 h after the snowfall.	Flin et al., 2004
I03	PP	4.91	62 h after the snowfall, under isothermal conditions at –2°C.	Flin et al., 2004
I04	PP	4.91	81 h after the snowfall, under isothermal conditions at –2°C.	Flin et al., 2004
I08	DF	4.91	297 h after the snowfall, under isothermal conditions at –2°C.	Flin et al., 2004
I15	RG	4.91	806 h after the snowfall, under isothermal conditions at –2°C.	Flin et al., 2004
I19	RG	4.91	1381 h after the snowfall, under isothermal conditions at –2°C.	Flin et al., 2004
I21	RG	4.91	1694 h after the snowfall, under isothermal conditions at –2°C.	Flin et al., 2004
I23	RG	4.91	2026 h after the snowfall, under isothermal conditions at –2°C.	Flin et al., 2004
P03	PP	8.48	Girose glacier[2], 20 cm depth, 17 March 2009.	Flin et al., 2011
P04	DF	8.588	Girose glacier, 40 cm depth, 17 March 2009.	Flin et al., 2011
P06	RG	6.158	Girose glacier, 60 cm depth, 17 March 2009.	Flin et al., 2011
P07	RG	8.609	Girose glacier, 70 cm depth, 17 March 2009.	Flin et al., 2011
P08	RG	8.552	Girose glacier, 100 cm depth, 17 March 2009.	Flin et al., 2011
P09	RG	6.158	Girose glacier, 120 cm depth, 17 March 2009.	Flin et al., 2011
P10	RG	6.103	Girose glacier, 165 cm depth, 17 March 2009.	Flin et al., 2011
P11	RG	8.588	Girose glacier, 65 cm depth, 1 March 2009.	Flin et al., 2011
P14	RG	6.154	Girose glacier, 80 cm depth, 1 March 2009.	Flin et al., 2011
P15	RG	6.158	Girose glacier, 170 cm depth, 1 March 2009.	Flin et al., 2011
H00	RG	8.609	Sieved snow, followed by isothermal conditions.	Flin et al., 2011
H01	MF	8.609	Grain coarsening of water-saturated snow and drainage after 1h.	Flin et al., 2011
H1-2	MF	8.590	Grain coarsening of water-saturated snow and drainage after 6h.	Flin et al., 2011
H02	MF	8.590	Grain coarsening of water-saturated snow and drainage after 24h.	Flin et al., 2011
H03	MF	8.609	Grain coarsening of water-saturated snow and drainage after 48h.	Flin et al., 2011
H05	MF	8.590	Grain coarsening of water-saturated snow and drainage after 142h.	Flin et al., 2011
Chamair	MF	10	Grain coarsening of water-saturated snow and drainage.	Coléou et al., 2001
E2b	FC	4.91	3 weeks under a TG = 16 K m^{-1}, T_{mean} = -3°C, sampled in the middle of the layer.	Flin et al., 2008
3A	DH	8.400	9 days under a TG = 43 K m^{-1}, T_{mean} = -4°C, sampled in the middle of the layer.	This study
4A	DH	8. 397	13 days under a TG = 43 K m^{-1}, T_{mean} = -4°C, sampled in the middle of the layer.	This study
Grad3	DH	10	8 days under a TG = 100 K m^{-1}, T_{mean} = -5°C.	Coléou et al., 2001

Table S1: List of the snow samples used in the present work. Snow type is defined according to the International Classification for Seasonal Snow on the Ground [*Fierz et al., 2009*]: PP, Precipitation Particles; DF, Decomposing and Fragmented precipitation particles; RG, Rounded Grains; FC, Faceted Crystals; DH, Depth Hoar; MF, Melt Forms. Lines with gray background correspond to samples for which detailed information is provided below.

[1] 1325 m altitude, Chartreuse range, France.
[2] 3200 m altitude, Ecrins range, France.

Sample *Fr* - Precipitation Particles (PP)

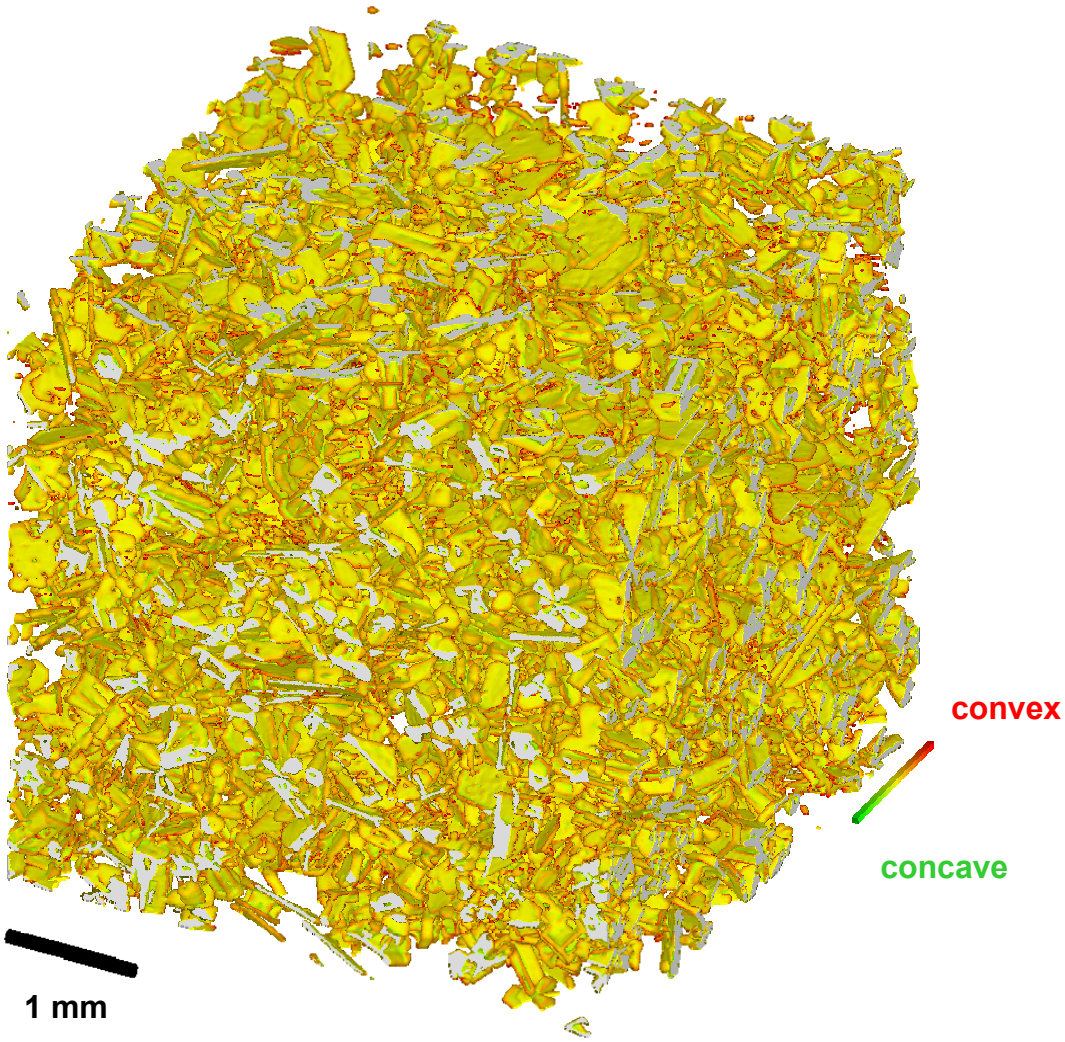

Figure S1a: 3D visualization of the microtomographic image (size = 1192^3 voxels, 1 vox. = 4.91 µm).

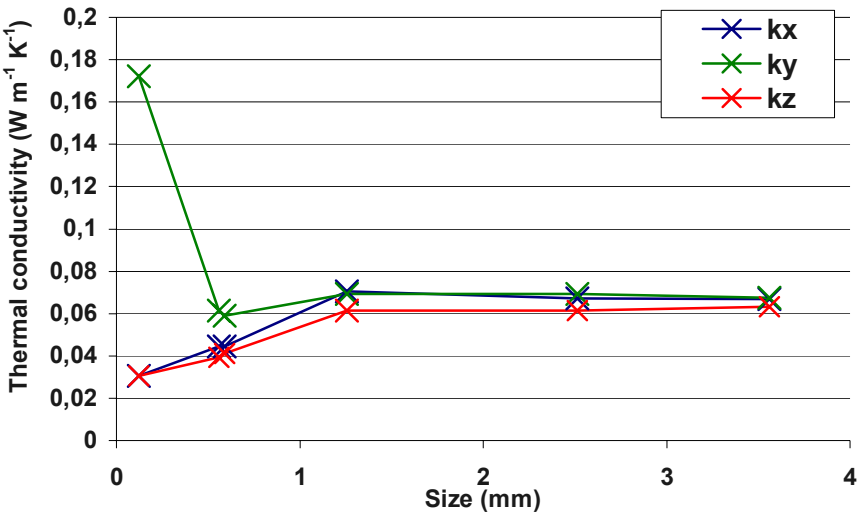

Figure S1b:
Dependency of k_{eff} estimates with sample size.

REV (mm)	**2.5**
Density (kg m^{-3})	**124.9**
k_x (W m^{-1} K^{-1})	**0.067**
k_y (W m^{-1} K^{-1})	**0.067**
k_z (W m^{-1} K^{-1})	**0.063**

Table S2:
Estimated REV, density and k_{eff} values.

Sample *P04* - Decomposing and Fragmented precipitation particles (DF)

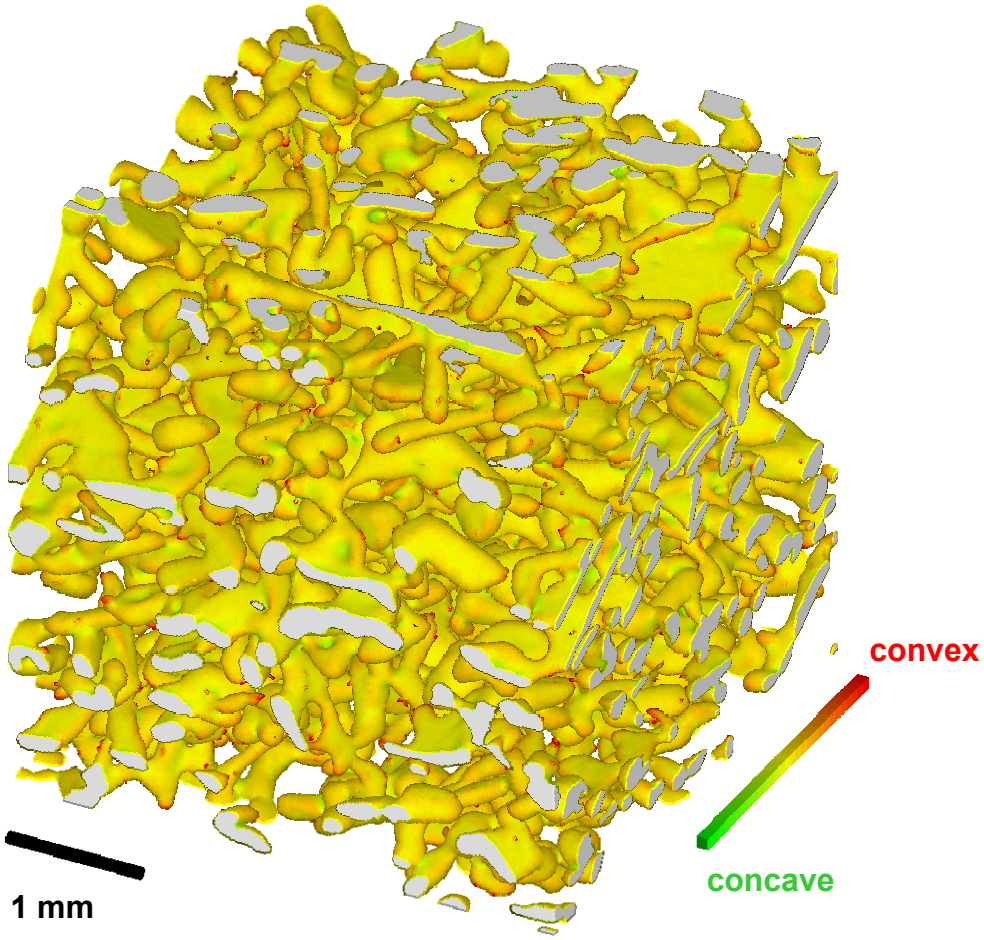

Figure S2a: 3D visualization of the microtomographic image (size = 512^3 voxels, 1 vox. = 8.588 µm).

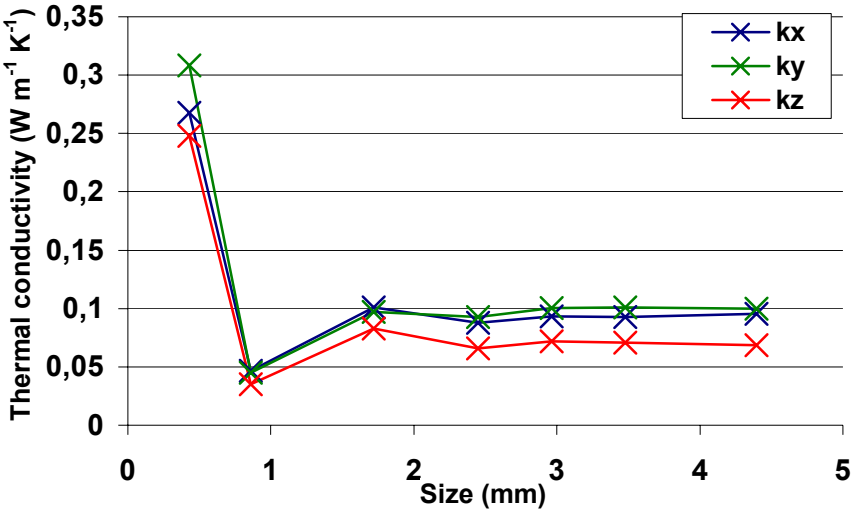

Figure S2b:
Dependency of k_{eff} estimates with sample size.

REV (mm)	**3**
Density (kg m^{-3})	**157.6**
k_X (W m^{-1} K^{-1})	**0.095**
k_Y (W m^{-1} K^{-1})	**0.100**
k_Z (W m^{-1} K^{-1})	**0.068**

Table S3:
Estimated REV, density and k_{eff} values.

Sample *P11* - Rounded Grains (RG)

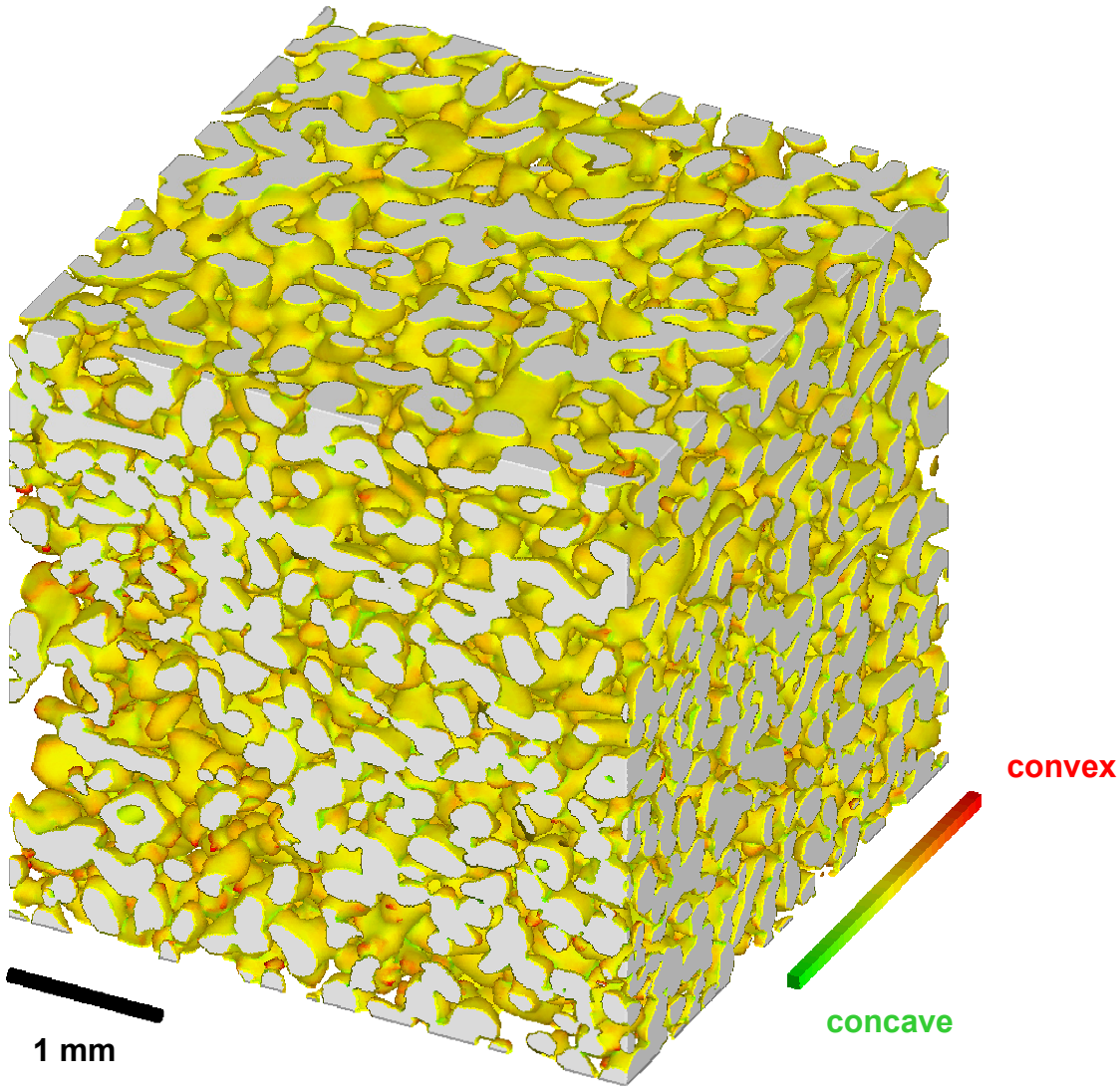

Figure S3a: 3D visualization of the microtomographic image (size = 512^3 voxels, 1 vox. = 8.588 µm).

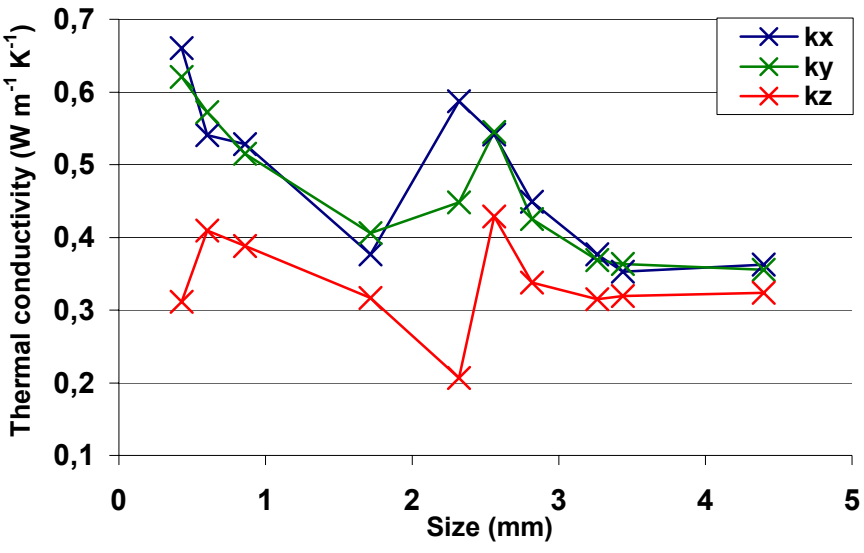

Figure S3b:
Dependency of k_{eff} estimates with sample size.

REV (mm)	**4**
Density (kg m^{-3})	**413.7**
k_X (W m^{-1} K^{-1})	**0.363**
k_Y (W m^{-1} K^{-1})	**0.356**
k_Z (W m^{-1} K^{-1})	**0.324**

Table S4:
Estimated REV, density and k_{eff} values.

Sample *H02* - Melt Forms (MF)

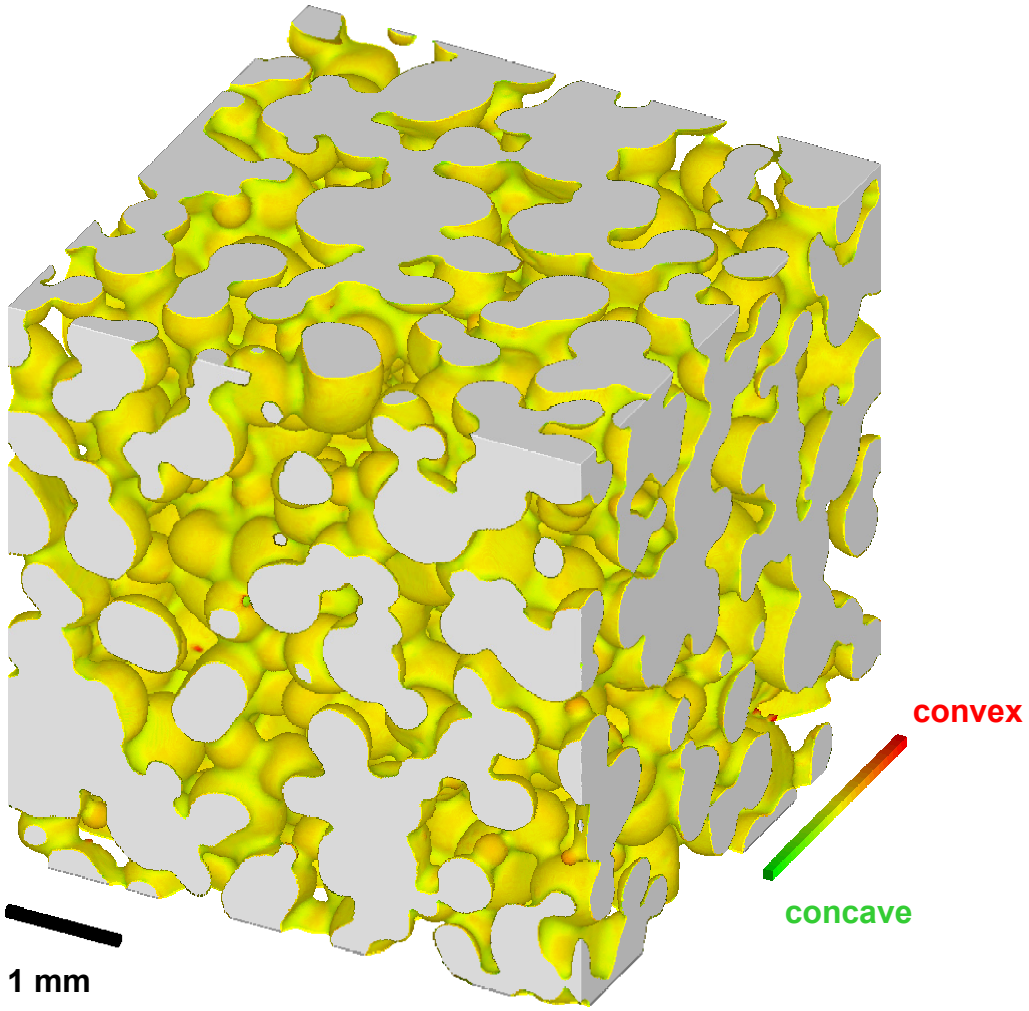

Figure S4a: 3D visualization of the microtomographic image (size = 651^3 voxels, 1 vox. = 8.590 µm).

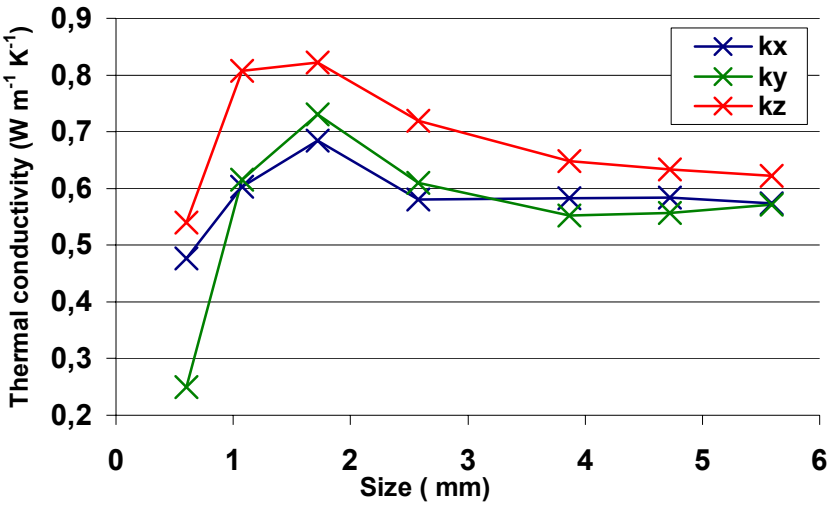

Figure S4b:
Dependency of k_{eff} estimates with sample size.

REV (mm)	**5.5**
Density (kg m^{-3})	**502.6**
k_x (W m^{-1} K^{-1})	**0.574**
k_y (W m^{-1} K^{-1})	**0.571**
k_z (W m^{-1} K^{-1})	**0.623**

Table S5:
Estimated REV, density and k_{eff} values.

Sample *E2b* – Faceted Crystals (FC)

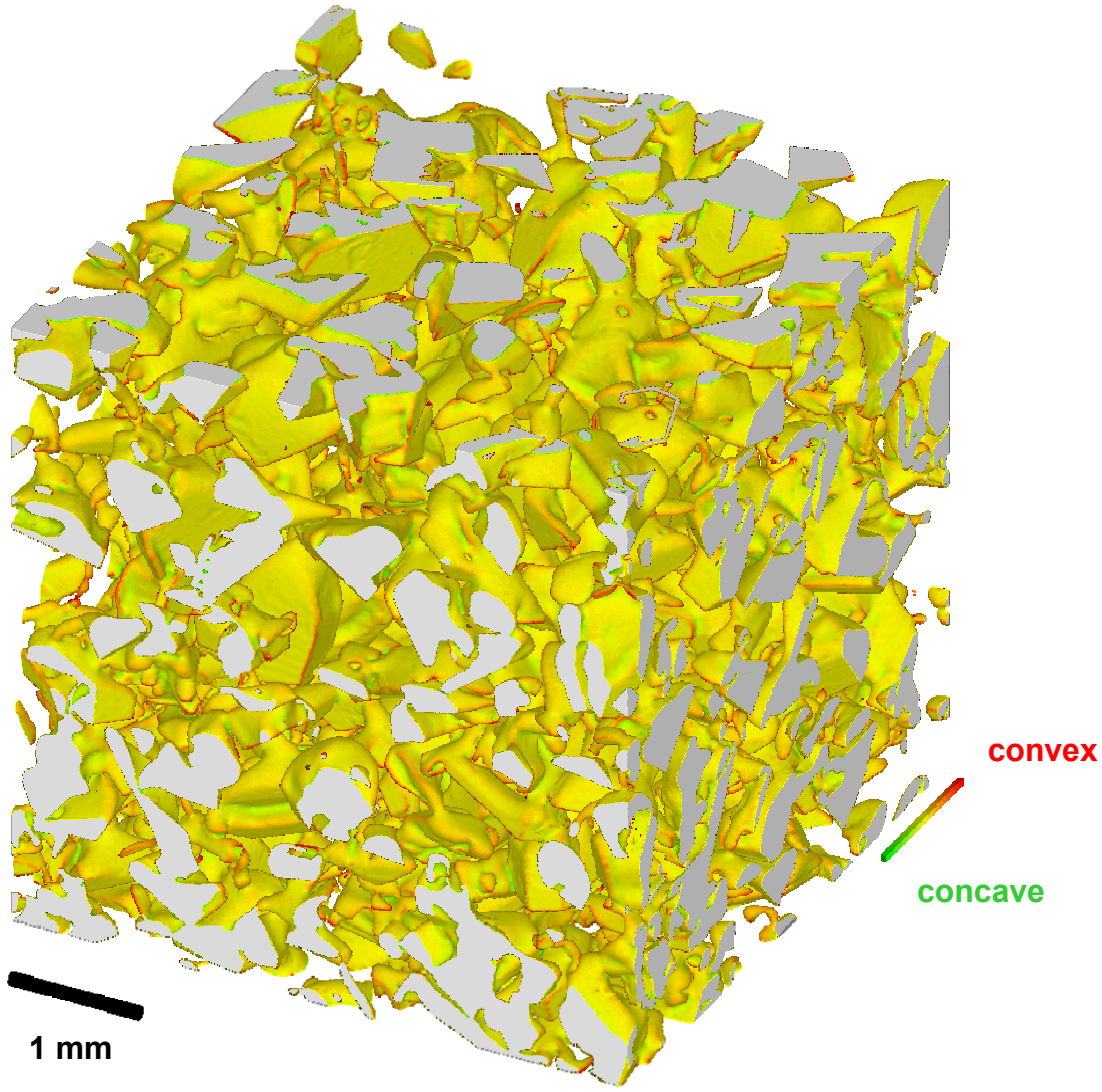

Figure S5: 3D visualization of the microtomographic image (size = 1200^3 voxels, 1 vox. = 4.91 µm).

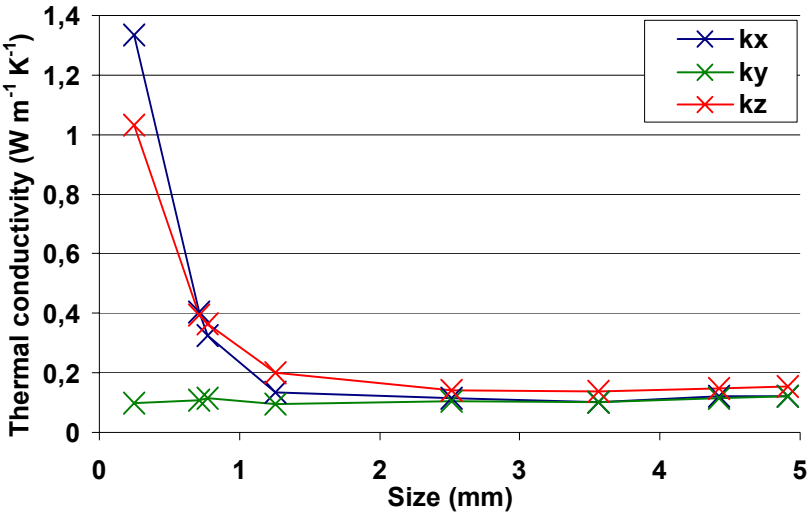

Figure S5b:
Dependency of k_{eff} estimates with sample size.

REV (mm)	**3**
Density (kg m^{-3})	**262.7**
k_x (W m^{-1} K^{-1})	**0.123**
k_y (W m^{-1} K^{-1})	**0.121**
k_z (W m^{-1} K^{-1})	**0.154**

Table S6:
Estimated REV, density and k_{eff} values.

Sample *Grad3* – Depth Hoar (DH)

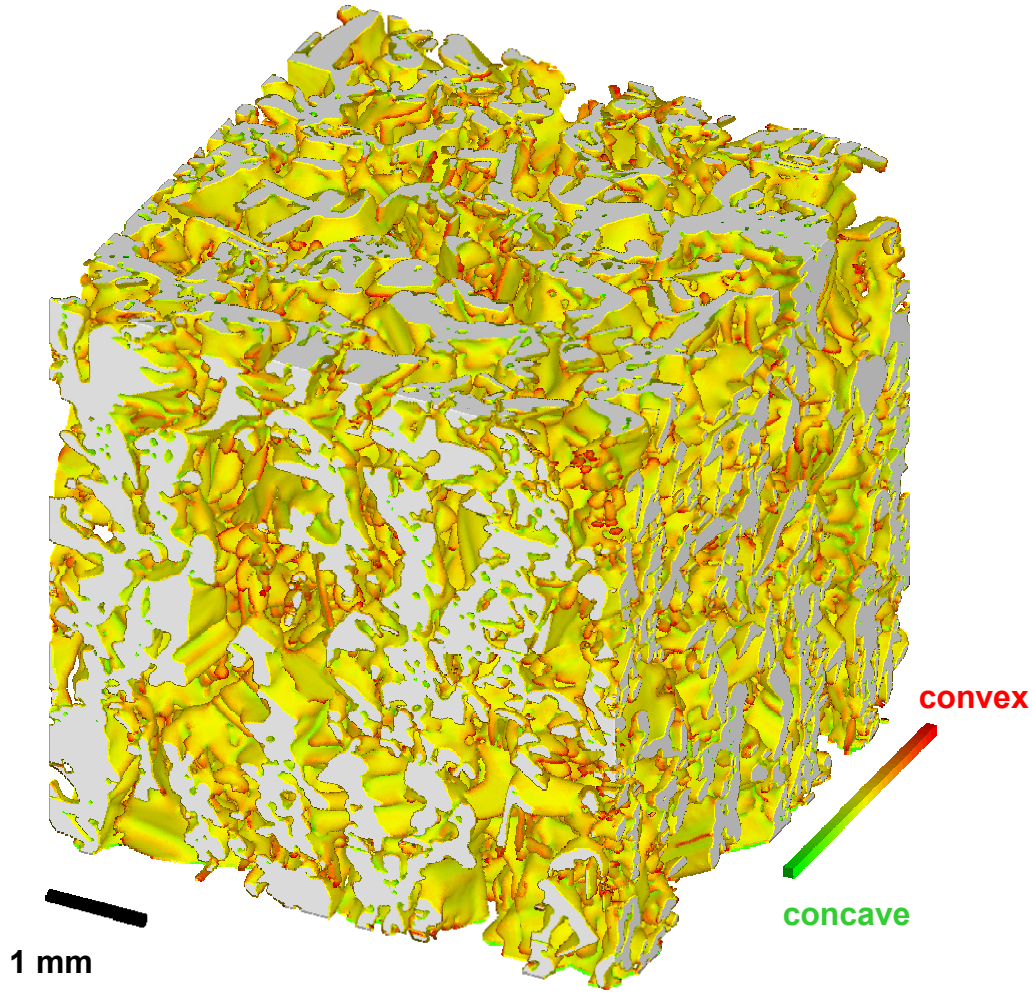

Figure S6a: 3D visualization of the microtomographic image (size = 600^3 voxels, 1 vox. = 10 µm).

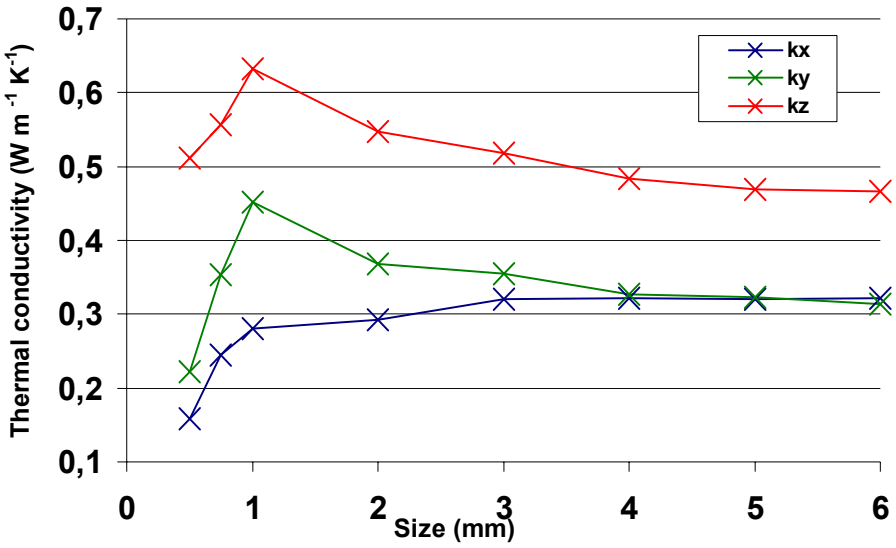

Figure S6b:
Dependency of k_{eff} estimates with sample size.

REV (mm)	**5**
Density (kg m^{-3})	**369.2**
k_X (W m^{-1} K^{-1})	**0.322**
k_Y (W m^{-1} K^{-1})	**0.314**
k_Z (W m^{-1} K^{-1})	**0.466**

Table S7:
Estimated REV, density and k_{eff} values.